Electronic Supplementary Material (ESI) for Physical Chemistry Chemical Physics

SUPPLEMENTARY INFORMATION

Shape-controlled TiO_2 nanoparticles and TiO_2 P25 interacting with CO and H_2O_2 molecular probes: a synergic approach for surface structure recognition and physico-chemical understanding

Chiara Deiana,[a,b] Marco Minella,[a] Gloria Tabacchi[b], Valter Maurino,[a] Ettore Fois[b] and Gianmario Martra[a]

[a] Department of Chemistry and Interdepartmental Centre of Excellence "Nanostructured Interfaces and Surfaces-NIS", University of Torino, via P. Giuria 7, 10125 Torino, Italy

[b] Dipartimento di Scienza ed Alta Tecnologia. University of Insubria and INSTM, via Lucini 3, 22100 Como, Italy.

Contents:

1) Complementary characterization methods and additional results

2) Theoretical modeling of CO adsorption

1) Complementary characterization methods and additional results

X-ray diffraction (XRD) pattern of the powders were recorded with an Analytical X'Pert Pro equipped with an X'Celerator detector powder diffractometer using Cu K_α radiation generated at 40 kV and 40 mA. The instrument was configured with 1/2° divergence and receiving slits. A quartz sample holder was used. The 2θ range was from 20° to 80° with a step size (°2θ) of 0.05 and a counting time of 3 s.

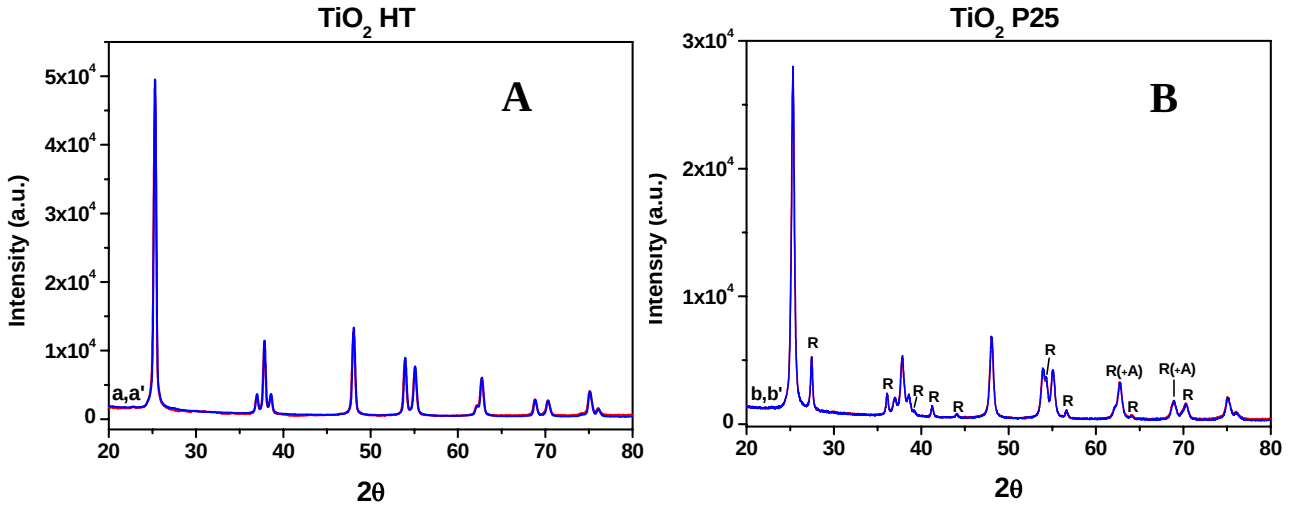

Figure S1. XRD patterns of TiO_2 HT (Panel A) and TiO_2 P25 (Panel B) as received (a, b, red lines) and after treatment at 873K (a',b', blue lines).

Comment to Figure S1:

The XRD patterns reported in Figure S1 show the presence of the only anatase phase for the TiO_2 HT sample (panel A), while, in the case of TiO_2 P25 (panel B), the presence of a mixture of anatase and rutile phases, typical for this material (~80% anatase, ~20% rutile) is observed.

The XRD patterns collected before and after the activation at 873 K are almost identical, thus indicating that no anatase-rutile phase transition has occurred at that temperature.

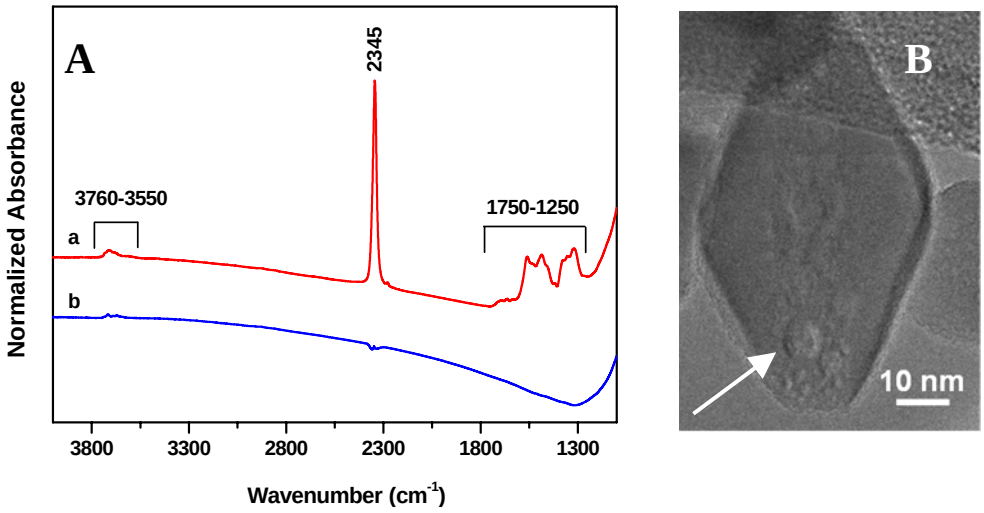

Figure S2. IR spectra of (a) TiO_2 HT and (b) TiO_2 P25 treated at 873 K as indicated in the IR measurement section. Panel B: TEM image of TiO_2 HT (original magnification x 200 k).

Comment to Figure S2:

After the treatment at 873 K, only signals related to OH groups at 3760-3550 cm^{-1} were observed for TiO_2 P25 sample; conversely, for the TiO_2 HT powder, also additional bands were present: an intense peak at 2345 cm^{-1}, due to the antisymmetric stretching mode of slightly perturbed CO_2 and a complex pattern in the 1750-1250 cm^{-1} range, typical of carboxylates/carbonates groups. The resistance of these species, resulting from the oxidation of organic moieties of the $Ti(TEOA)_2$ complex used for the synthesis, to the thermal treatment indicates that they should be entrapped in/at the inner surface of cavities present in the material (TEM image in panel B).

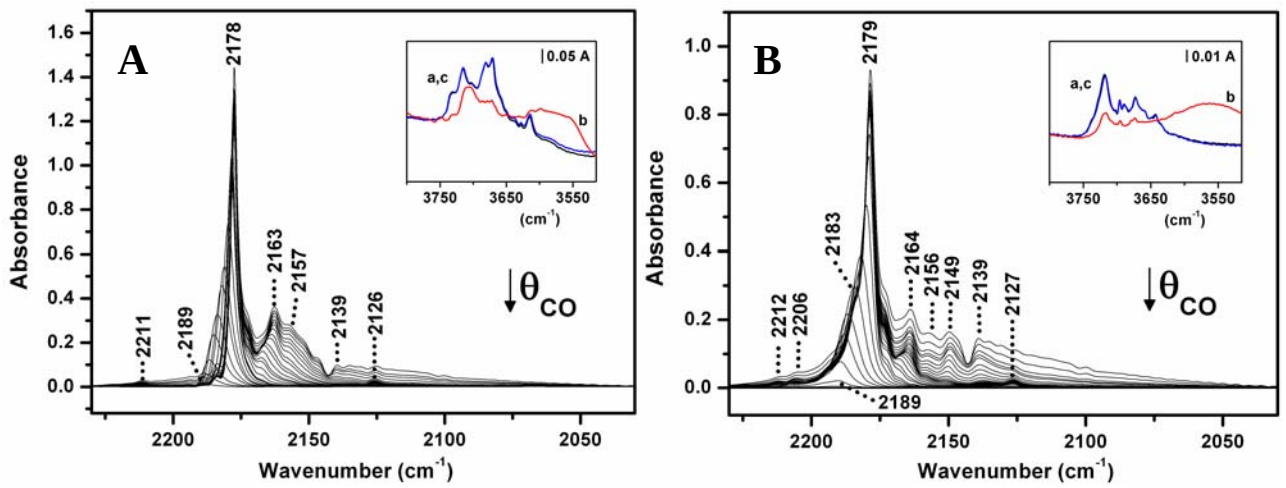

Figure S3. IR spectra of CO adsorbed at ca. 100 K on (A) TiO_2 HT and (B) TiO_2 P25 outgassed at 873 K. Spectra acquired at decreasing coverages (θ), from 45 mbar CO to outgassing for 10 min at ca. 100 K. Panel B adapted from the Supporting Information of ref.[1] Insets: IR spectra in the νOH region (a) before interaction with CO, (b) in contact with 45 mbar of CO, (c) in contact with 0.5 mbar of CO.

Comment to Figure S3:

As can be observed in Figure S3, the CO adsorption at 100 K on the surface of the two materials results in different signals in the IR spectra. The components below 2170 cm^{-1} preferentially decrease in intensity by removing the adsorbed CO, thus indicating a weaker interaction of CO molecules with adsorbing Ti^{4+} surface sites. The most intense peak at 2178/2179 cm^{-1} (for TiO_2 HT and TiO_2 P25, respectively) shifts to ca. 2189 cm^{-1} by decreasing the CO coverage (θ → 0), which usually results from the weakening of interactions among parallel and close oscillators.[2,3]

The partner signal due to ^{13}CO present in natural abundance appears at 2126/2127 cm^{-1}. In case of TiO_2 P25 a component at 2206 cm^{-1} is also present, showing a lower reversibility, in respect with the main peak at 2179 cm^{-1}, thus indicating a strong interaction of CO molecules adsorbed on surface sites responsible for this signal.

The component at 2157/2156 cm^{-1} is due to stretching of CO molecules interacting with the residual surface hydroxy groups present after outgassing at 873 K. The perturbation of the νOH signals as a consequence of the interaction with CO, is reported in the inset of Figure S3 A and B for TiO_2 HT and TiO_2 P25, respectively. In the literature there is a general consensus on assigning νOH signals at $\nu < 3680$ cm^{-1} to bridged hydroxy groups, and νOH signals at higher frequencies to linear

species.[1] As can be observed, the signals present in spectrum a before CO adsorption, are shifted to lower frequency and produce a broad band, when in contact with CO (curve b). After desorption of CO the original νOH profiles is restored (curve c, inset).

Details on the assignment of the different bands present in the IR spectra of adsorbed CO on these TiO_2 materials are reported in the main text.

References

(1) Deiana C., Fois E., Coluccia S., Martra G., *J. Phys. Chem. C.* **2010**, *114*, 21531-21538, and references therein.
(2) Hadjiivanov K., Lamotte J., Lavalley J. C., *Langmuir* **1997**, *13*, 3374-3381.
(3) Hadjiivanov K., Vayssilov G. N., *Adv. Catal.* **2002**, *47*, 307-511.

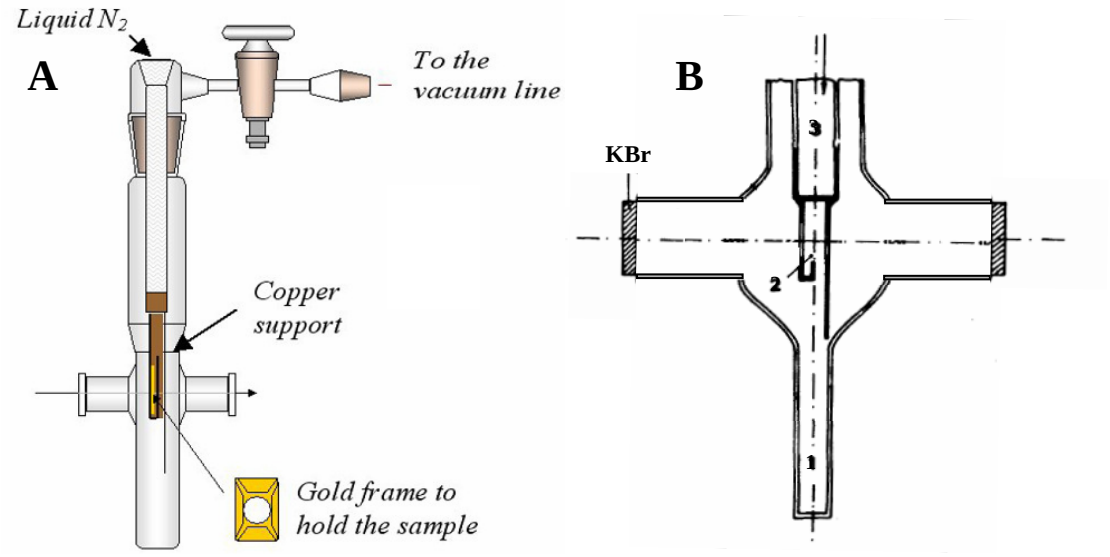

Figure S4. Panel A: scheme of the cell used to carry out infrared measurements at ca. 100 K (reprinted with permission from ref. 1). Panel B: zoomed view of the terminal part of the cell (adapted from ref. 2 with permission from The Royal Society of Chemistry).

Comment to Figure S4 (adapted with permission from ref 2):

The cell used in this study is of the same type as the one described in ref 2, used in our laboratory since twenty years. It allows both thermal treatments (up to 1173 K) and low-temperature (ca. 100 K) adsorption-desorption experiments to be carried out *in situ*. The sample is thermally treated in position 1, by means of an external furnace, while the other parts of the cell are kept at room temperature by a flow of air. Subsequently, the sample is transferred to position 2. Liquid nitrogen is then fed into the Kovar-Pyrex tubing, 3.

References

(1) Chapter 5 "Surface Characterization of Inorganic Nanobiomaterials at a Molecular Scale: Use of Vibrational Spectroscopies" (pp. 153-172), by Martra G., Aina V., Sakhno Y., Bertinetti L., Morterra C., of the E-Book "Surface Tailoring of Inorgainc Materials for Biomedical Applications" edited by Rimondini L., Bianchi B. and Verné E., Bentham E-books, eISBN: 978-1-60805-462-6, **2012**.
(2) Marchese L., Bordiga S., Coluccia S., Martra G., Zecchina A., *J. Chem. Soc. Faraday Trans.* **1993**, *89*, 3483-3489.

2) Theoretical Modeling of CO adsorption

Table S1a. Cutoff dependence of the two inequivalent Ti-O distances ($Ti-O_1$, $Ti-O_2$) in anatase. Calculations performed with fixed cell parameters (11.355×11.355×9.514 $Å^3$), corresponding to 3×3×1 crystallographic unit cells, and with a (2×2×2) Monkorst-Pack mesh. Cutoff (1st column) in Ry, distances in Å.

Cutoff ((2×2×2) BZ)	$Ti-O_1$	$Ti-O_2$
70	2.0016	1.9297
80	1.9803	1.9339
90	1.9823	1.9335
100	1.9828	1.9334
110	1.9829	1.9334
120	1.9829	1.9334
Exp	1.9795	1.9341

Table S1b. Cutoff dependence of the two inequivalent Ti-O distances in anatase. Calculations performed at Γ with fixed cell parameters (11.355×11.355×9.514$Å^3$) corresponding to 3×3×1 crystallographic unit cells. Cutoff (1st column) in Ry, distances in Å.

Cutoff (Γ)	$Ti-O_1$	$Ti-O_2$
70	2.0085	1.9283
80	1.9854	1.9330
90	1.9872	1.9325
100	1.9875	1.9325
110	1.9875	1.9325
120	1.9854	1.9329
Exp	1.9795	1.9341

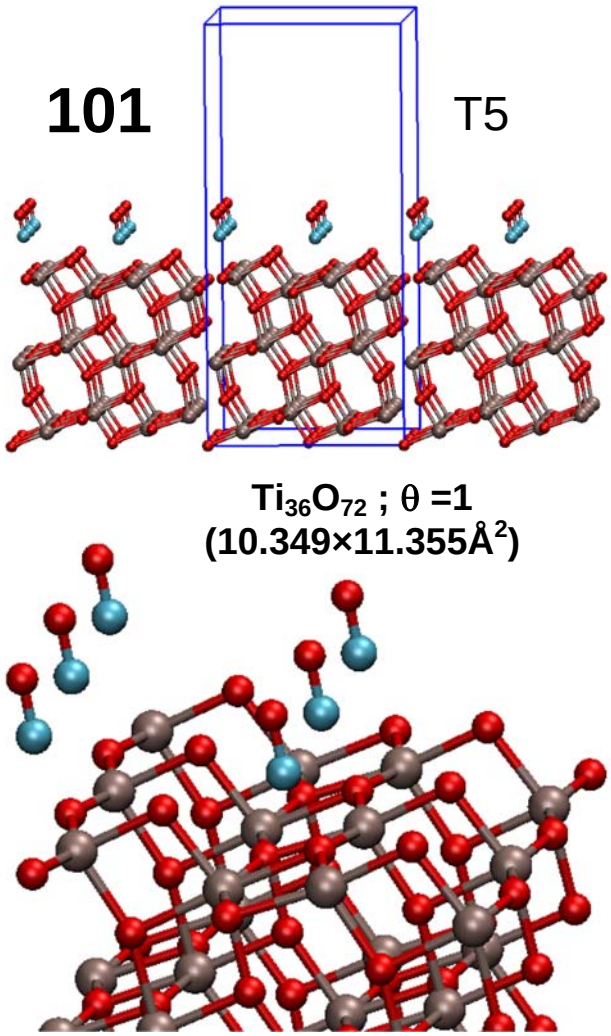

Figure S5a. Ball-and-stick representation of CO on (101) model slab at θ=1. Color code: Ti atoms are represented as gray spheres, O atoms as red spheres, C atoms as cyan spheres. The blue lines represent the simulation cell.

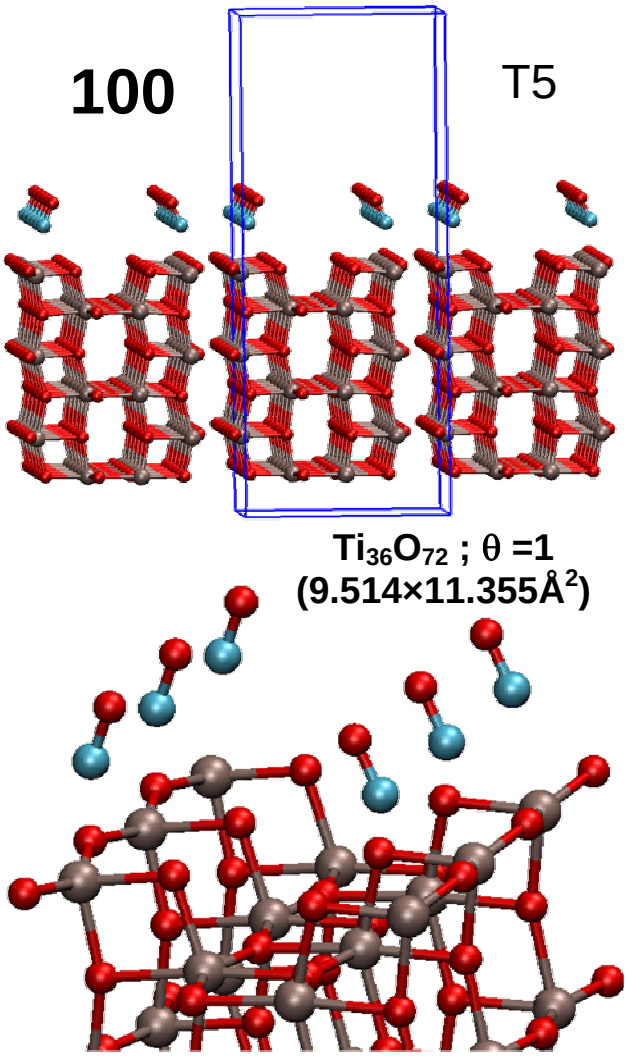

Figure S5b. Ball-and-stick representation of CO on (100) model slab at θ=1. Color code: Ti atoms are represented as gray spheres, O atoms as red spheres, C atoms as cyan spheres. The blue lines represent the simulation cell.

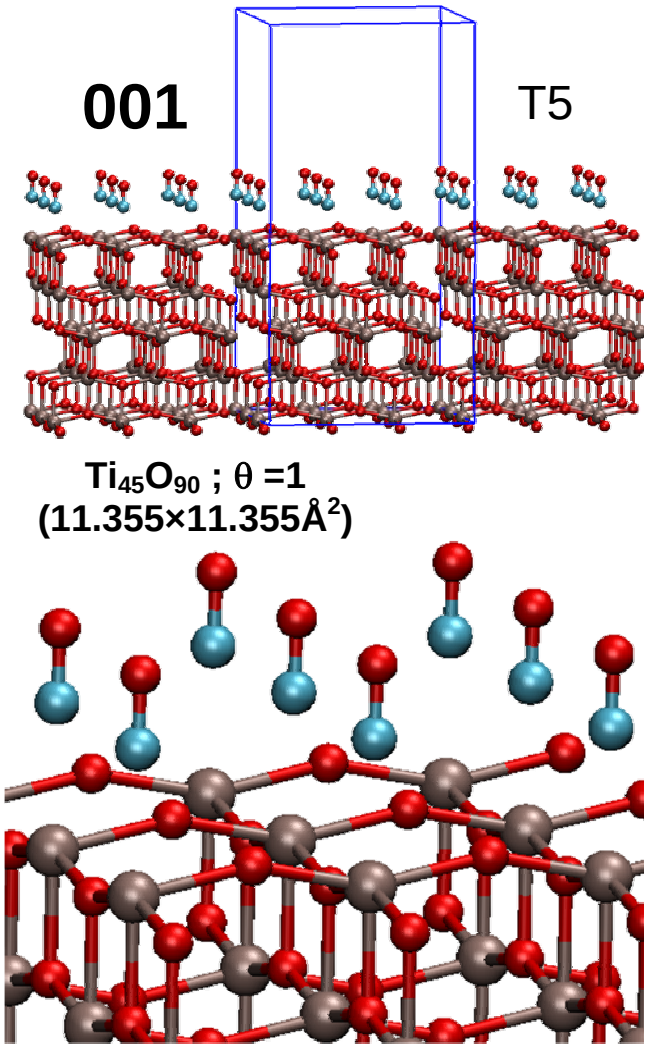

Figure S5c. Ball-and-stick representation of CO on (001) model slab at θ=1. Color code: Ti atoms are represented as gray spheres, O atoms as red spheres, C atoms as cyan spheres. The blue lines represent the simulation cell.

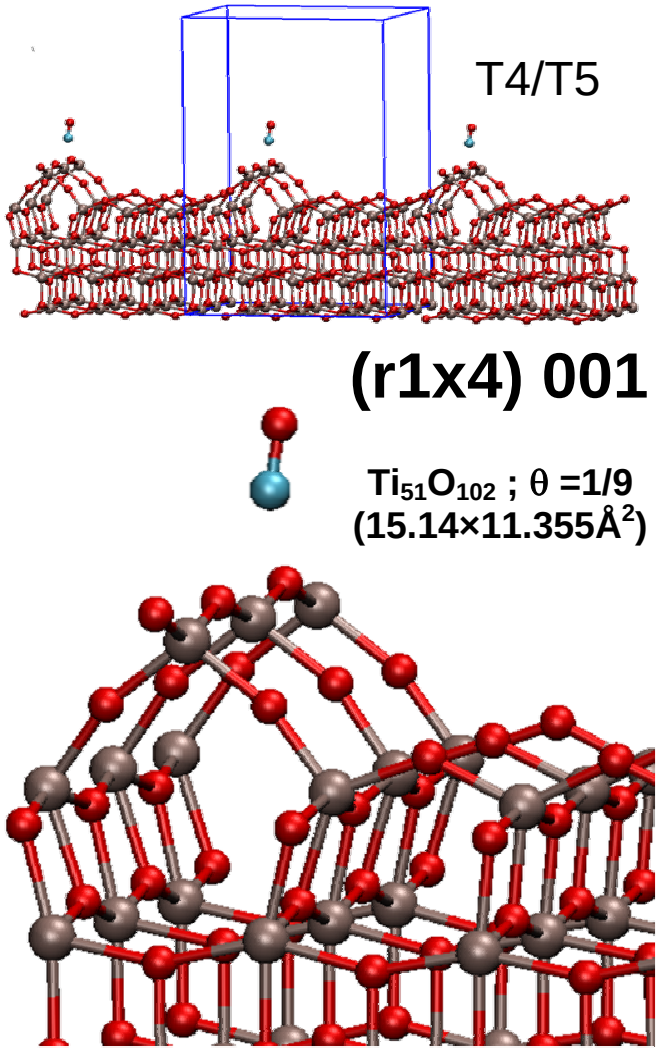

Figure S5d. Ball-and-stick representation of one CO molecule on r1x4 (001) model slab. Color code: Ti atoms are represented as gray spheres, O atoms as red spheres, C atoms as cyan spheres. The blue lines represent the simulation cell.

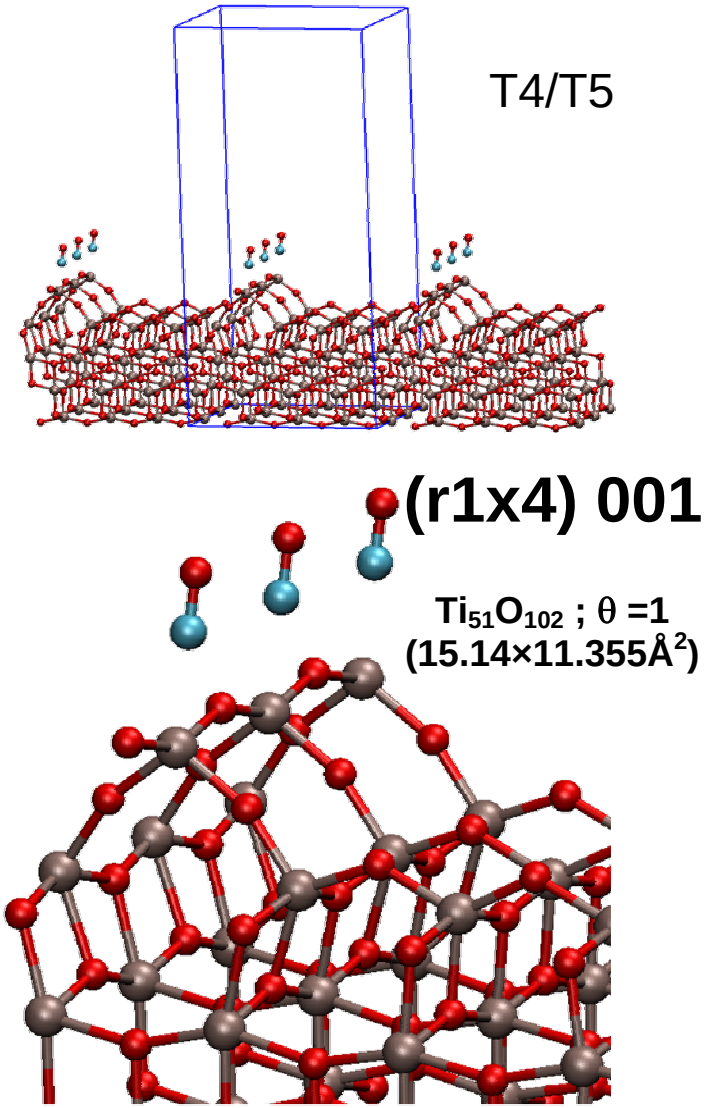

Figure S5e. Ball-and-stick representation of three CO molecules on r1x4 (001) model slab. Color code: Ti atoms are represented as gray spheres, O atoms as red spheres, C atoms as cyan spheres. The blue lines represent the simulation cell.

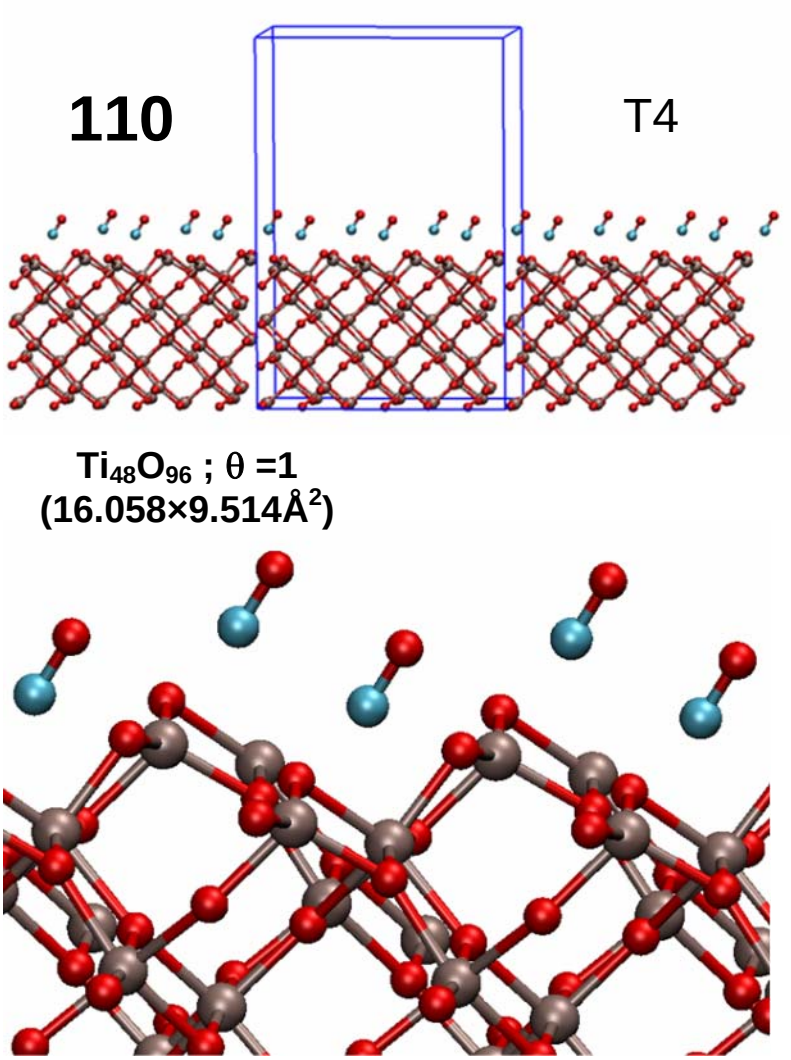

Figure S5f. Ball-and-stick representation of CO on (110) model slab at θ=1. Color code: Ti atoms are represented as gray spheres, O atoms as red spheres, C atoms as cyan spheres. The blue lines represent the simulation cell.

Table S2a. Calculated CO stretching modes and corresponding frequencies for the simulated CO/(101) TiO_2 anatase model systems (θ=1 conditions). Since the ^{13}CO band can be unambiguously assigned from the experimental spectra, the ratio between the experimental $\nu^{13}CO$ (2126 cm^{-1}) and the calculated $\nu^{13}CO$ for thermally and chemically disordered ^{13}CO/(101) (2101.3 cm^{-1}) was adopted as scaling factor.

TiO_2 (101) surface			
Type of disorder and compositon of the adsorbate	Mode	Calculated νCO [cm^{-1}]	Scaled νCO [cm^{-1}]
Ordered: 6 ^{12}CO	ν ^{12}CO	2162.9	2188.3
Chemical Disorder: 5 ^{12}CO+ 1 ^{13}CO	ν_1 ^{12}CO	2138.8	2163.9
	ν_2 ^{12}CO	2139.3	2164.4
	ν_3 ^{12}CO	2139.9	2165.0
	ν_4 ^{12}CO	2142.0	2167.1
	ν_5 ^{12}CO	2148.1	2173.3
	ν_6 ^{13}CO	2093.9	2118.5
Thermal Disorder: 6 ^{12}CO	ν_1 ^{12}CO	2146.3	2171.5
	ν_2 ^{12}CO	2146.4	2171.6
	ν_3 ^{12}CO	2147.0	2172.2
	ν_4 ^{12}CO	2147.1	2172.3
	ν_5 ^{12}CO	2150.3	2175.5
	ν_6 ^{12}CO	2155.0	2180.3
Thermal and Chemical Disorder: 5 ^{12}CO+ 1 ^{13}CO	ν_1 ^{12}CO	2146.4	2171.6
	ν_2 ^{12}CO	2146.9	2172.1
	ν_3 ^{12}CO	2147.2	2172.4
	ν_4 ^{12}CO	2149.7	2175.0
	ν_5 ^{12}CO	2154.8	2180.1
	ν_6 ^{13}CO	2101.3	2126.0

Table S2b. Calculated CO stretching modes and corresponding frequencies for the simulated CO/(100) TiO_2 anatase model systems (θ=1 conditions). Since the ^{13}CO band can be unambiguously assigned from the experimental spectra, the ratio between the experimental $\nu^{13}CO$ (2126 cm^{-1}) and the calculated $\nu^{13}CO$ for thermally and chemically disordered ^{13}CO/(101) (2101.3 cm^{-1}) was adopted as scaling factor.

TiO_2 (100) surface			
Type of disorder and compositon of the adsorbate	Mode	Calculated νCO [cm^{-1}]	Scaled νCO [cm^{-1}]
Ordered: 6 ^{12}CO	ν_1 ^{12}CO	2138.2	2163.3
	ν_2 ^{12}CO	2128.2	2153.2
Chemical Disorder: 5 ^{12}CO+ 1 ^{13}CO	ν_1 ^{12}CO	2122.5	2147.4
	ν_2 ^{12}CO	2125.6	2150.5
	ν_3 ^{12}CO	2126.1	2151.1
	ν_4 ^{12}CO	2126.4	2151.3
	ν_5 ^{12}CO	2136.3	2161.4
	ν_6 ^{13}CO	2078.0	2102.4
Thermal Disorder: 6 ^{12}CO	ν_1 ^{12}CO	2123.8	2148.8
	ν_2 ^{12}CO	2124.0	2148.9
	ν_3 ^{12}CO	2126.1	2151.1
	ν_4 ^{12}CO	2126.2	2151.1
	ν_5 ^{12}CO	2127.7	2152.7
	ν_6 ^{12}CO	2138.2	2163.3
Thermal and Chemical Disorder: 5 ^{12}CO+ 1 ^{13}CO	ν_1 ^{12}CO	2123.9	2148.8
	ν_2 ^{12}CO	2125.4	2150.3
	ν_3 ^{12}CO	2126.1	2151.1
	ν_4 ^{12}CO	2127.1	2152.1
	ν_5 ^{12}CO	2136.4	2161.5
	ν_6 ^{13}CO	2079.7	2104.1

In the case of CO adsorbed on the TiO_2 (100) facet at θ=1, two CO stretching frequencies are calculated for the ordered structure. Indeed, CO on (100) is arranged in a 2×1 pattern, as shown in Figure S5b: for such a structure, a splitting of 10 cm^{-1} is calculated. νCO splitting has been also reported for CO adsorbed on MgO at temperatures below 45 K in Heidberg J., Kandel M., Meine D., Wildt U. *Surf. Sci.* **1995**, *331*, pp 1467-1472.

Table S2c. Calculated CO stretching modes and corresponding frequencies for the simulated CO/(001) TiO_2 anatase model systems (θ=1 conditions) and CO/(001) reconstructed (θ=1 and θ=1/3 conditions). Since the ^{13}CO band can be unambiguously assigned from the experimental spectra, the ratio between the experimental $\nu^{13}CO$ (2126 cm^{-1}) and the calculated $\nu^{13}CO$ for thermally and chemically disordered ^{13}CO/(101) (2101.3 cm^{-1}) was adopted as scaling factor.

TiO_2 (001) surface			
Ordered: 9 ^{12}CO	ν ^{12}CO	2112.6	2137.4
Chemical Disorder: 8 ^{12}CO+ 1 ^{13}CO	ν_1 ^{12}CO	2112.2	2137.0
	ν_2 ^{12}CO	2097.6	2122.2
	ν_3 ^{12}CO	2097.0	2121.6
	ν_4 ^{12}CO	2096.2	2120.8
	ν_5 ^{12}CO	2093.3	2117.9
	ν_6 ^{12}CO	2090.9	2115.4
	ν_7 ^{12}CO	2090.9	2115.4
	ν_8 ^{12}CO	2090.8	2115.3
	ν_9 ^{13}CO	2048.5	2072.5
Thermal Disorder: 9 ^{12}CO	ν_1 ^{12}CO	2109.3	2134.1
	ν_2 ^{12}CO	2093.1	2117.7
	ν_3 ^{12}CO	2092.9	2117.5
	ν_4 ^{12}CO	2091.7	2116.3
	ν_5 ^{12}CO	2090.8	2115.3
	ν_6 ^{12}CO	2086.5	2111.0
	ν_7 ^{12}CO	2086.3	2110.8
	ν_8 ^{12}CO	2085.7	2110.2
	ν_9 ^{12}CO	2085.5	2110.0
Thermal and Chemical Disorder: 8 ^{12}CO+ 1 ^{13}CO	ν_1 ^{12}CO	2043.5	2067.5
	ν_2 ^{12}CO	2093.3	2117.9
	ν_3 ^{12}CO	2092.6	2117.2
	ν_4 ^{12}CO	2091.9	2116.5
	ν_5 ^{12}CO	2089.3	2113.8
	ν_6 ^{12}CO	2086.8	2111.3
	ν_7 ^{12}CO	2086.4	2110.9
	ν_8 ^{12}CO	2085.9	2110.4
	ν_9 ^{13}CO	2018.2	2041.9
R(1×4) 3 ^{12}CO (on T(4))	ν ^{12}CO	2128.2	2153.2
R(1×4) 1 ^{12}CO (on T(4))	ν ^{12}CO	2143.4	2168.6

Table S2d. Calculated CO stretching modes and corresponding frequencies for the simulated CO/(110) TiO_2 anatase model systems (θ=1 conditions). Since the ^{13}CO band can be unambiguously assigned from the experimental spectra, the ratio between the experimental $\nu^{13}CO$ (2126 cm^{-1}) and the calculated $\nu^{13}CO$ for thermally and chemically disordered ^{13}CO/(101) (2101.3 cm^{-1}) was adopted as scaling factor.

TiO_2 (110) Surface			
Ordered: 6 ^{12}CO	ν ^{12}CO	2159.6	2184.9
Chemical Disorder: 5 ^{12}CO+ 1 ^{13}CO	ν_1 ^{12}CO	2157.5	2182.8
	ν_2 ^{12}CO	2155.8	2181.1
	ν_3 ^{12}CO	2152.5	2177.8
	ν_4 ^{12}CO	2152.3	2177.6
	ν_5 ^{12}CO	2148.8	2174.0
	ν_6 ^{13}CO	2101.8	2126.5
Thermal Disorder: 6 ^{12}CO	ν_1 ^{12}CO	2158.4	2183.7
	ν_2 ^{12}CO	2155.6	2180.9
	ν_3 ^{12}CO	2154.9	2180.2
	ν_4 ^{12}CO	2153.5	2178.8
	ν_5 ^{12}CO	2152.9	2178.2
	ν_6 ^{12}CO	2152.6	2177.9
Thermal and Chemical Disorder: 5 ^{12}CO+ 1 ^{13}CO	ν_1 ^{12}CO	2159.0	2184.3
	ν_2 ^{12}CO	2156.3	2181.6
	ν_3 ^{12}CO	2155.5	2180.8
	ν_4 ^{12}CO	2154.2	2179.5
	ν_5 ^{12}CO	2153.0	2178.3
	ν_6 ^{13}CO	2108.5	2133.2